Northumbria Research Link

University**Library**

Cruz Viggi C, Matturro B, Frascadore E, Insogna S, Mezzi A, Kaciulis S, Sherry A, Mejeha OK, Head IM, Vaiopoulou E, Rabaey K, Rossetti S, Aulenta F.

Bridging spatially segregated redox zones with a microbial electrochemical snorkel triggers biogeochemical cycles in oil-contaminated River Tyne (UK) sediments.

1 **Bridging spatially segregated redox zones with a microbial electrochemical**

2 **snorkel triggers biogeochemical cycles in oil-contaminated River Tyne (UK)**

3 **sediments**

4

5 Carolina Cruz Viggi[1], Bruna Matturro[1], Emanuela Frascadore[1], Susanna Insogna[2],

6 Alessio Mezzi[3], Saulius Kaciulis[3], Angela Sherry[4], Obioma K. Mejeha[4], Ian M. Head[4], Eleni

7 Vaiopoulou[5], Korneel Rabaey[5], Simona Rossetti[1], Federico Aulenta[1,*]

8

9

10 [1] Water Research Institute (IRSA), National Research Council (CNR), Italy

11 [2] Department of Chemistry, Sapienza University of Rome, Italy

12 [3] Institute for the Study of Nanostructured Materials (ISMN), National Research

13 Council (CNR), Italy

14 [4] School of Civil Engineering and Geosciences, Newcastle University, United

15 Kingdom

16 [5] Center for Microbial Ecology and Technology (CMET), Ghent University,

17 Belgium

18

19 [*] Corresponding Author

20 E-mail: Aulenta@irsa.cnr.it; Tel: +39-0690672751; Fax: +39-0690672787

21 Address: IRSA-CNR, Via Salaria km 29,300, 00015 Monterotondo (RM), Italy

22

23 **Abstract**

24 Marine sediments represent an important sink for a number of anthropogenic organic

25 contaminants, including petroleum hydrocarbons following an accidental oil spill.

26 Degradation of these compounds largely depends on the activity of sedimentary

27 microbial communities linked to biogeochemical cycles, in which abundant elements

28 such as iron and sulfur are shuttled between their oxidized and reduced forms. Here we

29 show that introduction of a small electrically conductive graphite rod ("the

30 electrochemical snorkel") into an oil-contaminated River Tyne (UK) sediment, so as to

31 create an electrochemical connection between the anoxic contaminated sediment and

32 the oxygenated overlying water, has a large impact on the rate of metabolic reactions

33 taking place in the bulk sediment. The electrochemical snorkel accelerated sulfate

34 reduction processes driven by organic contaminant oxidation and suppressed

35 competitive methane-producing reactions. The application of a comprehensive suite of

36 chemical, spectroscopic, biomolecular and thermodynamic analyses suggested that the

37 snorkel served as a scavenger of toxic sulfide via a redox interaction with the iron cycle.

38 Taken as a whole, the results of this work highlight a new strategy for manipulating

39 biological processes, such as bioremediation, corrosion, and carbon sequestration,

40 through the manipulation of the electron flows in contaminated sediments.

41

42 **Keywords**: Contaminated sediments, Iron cycle, Electrochemical snorkel, Oil spill

43 remediation, Petroleum hydrocarbons, Sulfate reduction, Sulfide scavenging, Sulfur

44 cycle

45

1.   Introduction

The release of thousands of tons of petroleum hydrocarbons (PHs) originating from anthropogenic activity affects the marine environment and causes severe ecological and economic damage (Bargiela et al., 2015). When an oil spill occurs, a variety of hydrocarbon removal strategies can be applied to minimize negative environmental impacts. Biological remediation methods are now widely used due to their lower environmental impact, adaptability to a range of contamination scenarios, and potential for full contaminant mineralization (Daghio et al., 2016). In confined hydrocarbon-rich environments, such as marine sediments, anoxic conditions prevail due to the excess of organic carbon that leads to rapid depletion of the most thermodynamically favorable electron acceptors (Bellagamba et al., 2016).

In anoxic sedimentary environments, the degradation of organic contaminants is usually stimulated by the addition of electron acceptors (e.g., oxygen, nitrate or sulfate) to provide microorganisms with more energetically favorable conditions for hydrocarbon oxidation (Meckenstock et al., 2004; Spormann and Widdel, 2000). Aerobic bioremediation is often favored over stimulation of anaerobic/anoxic contaminant degradation processes due to faster rates of hydrocarbon activation and removal (Viggi et al., 2015). In this context, a number of different approaches have been proposed to effectively deliver oxygen to contaminated anoxic sediments in order to accelerate hydrocarbon biodegradation (Genovese et al., 2014). However, rapid abiotic consumption of oxygen by reaction with reduced chemical species (e.g., Fe^{2+}, S^{2-}) and difficulties in controlling the rate of oxygen release limit the practical application of these approaches.

An alternative approach to overcoming electron acceptor limitation in oil-contaminated sediments is the use of bioelectrochemical systems (BES) (Lovley and Nevin, 2011;

71 Wang and Ren, 2013). BES employ solid-state electrodes to directly or indirectly

72 stimulate and control microbial metabolism. Stimulation of microbial activity is driven

73 by the ability of "electro-active bacteria" (EAB) to exchange electrons with the

74 electrodes, which can serve as electron acceptors or donors in their energy metabolism

75 (Borole et al., 2011). Recent, laboratory-scale studies have demonstrated that BES-based

76 technologies can be successfully applied to remove hydrocarbons from oil-contaminated

77 sediments (Bellagamba et al., 2016; Daghio et al., 2016; Morris et al., 2009; Yan and

78 Reible, 2014).

79 The concept of bioelectrochemical bioremediation to accelerate hydrocarbons

80 biodegradation in anoxic marine sediment was introduced recently (Viggi et al., 2015).

81 The system was based on an "Oil-spill Snorkel" consisting of a rod of conductive material

82 (i.e., an electrode) positioned to create an electrochemical connection between the

83 anoxic contaminated sediment and the oxic overlying water. In principle, the snorkel

84 could take advantage of the capability of EAB to anaerobically oxidize hydrocarbons

85 with a carbon electrode, deployed in the sediment, serving as a respiratory electron

86 acceptor. The electrons travel from the bottom of the snorkel buried in the sediment

87 (anode) to the upper part of the snorkel immersed in the overlying oxic water (cathode)

88 where oxygen is reduced to water, effectively spatially separating the oxidation of the

89 electron donor (hydrocarbons) from the reduction of the terminal electron acceptor.

90 Collectively, the results of this preliminary study confirmed the potential of the snorkel

91 to accelerate biotic and abiotic oxidative reactions taking place within the sediment, as

92 documented by a 1.7-fold increase in the cumulative oxygen uptake and 1.4-fold

93 increase in the cumulative CO_2 evolution, in microcosms containing snorkels compared

94 to snorkel-free controls. Accordingly, the initial rate of petroleum hydrocarbon

95 biodegradation was also substantially enhanced (Viggi et al., 2015). Despite these

96 promising findings, the fundamental mechanisms underlying the observed enhancement

97 of hydrocarbon degradation could not be identified and the overall impact of the

98 microbial electrochemical snorkel on key sediment biogeochemical cycles were not

99 elucidated. To gain a deeper understanding of these critical factors, further oil-spill

100 snorkel experiments were conducted using petroleum-contaminated estuarine

101 sediments from the River Tyne (UK) which had been previously reported to harbor

102 active sulfate-reducing, and syntrophic methanogenic hydrocarbon-degrading microbial

103 communities (O'Sullivan et al., 2015; Sherry et al., 2014).

104

105

106 **2.   Materials and Methods**

107 *2.1   Experimental setup*

108 The experiments described below are hereafter referred to as oil–spill snorkel

109 experiments. The estuarine sediments used in this study were obtained from the River

110 Tyne (UK). Sediment samples were subject to four treatments; 1) oil-supplemented

111 sediment containing 3 graphite rods, termed "snorkel", 2) sediment with no oil

112 amendment containing 3 graphite rods, termed "no oil snorkel", 3) oil-supplemented

113 sediment without graphite rods, termed "control", and 4) sediment with no oil

114 amendment or graphite rods, termed "no oil control". The oil containing treatments

115 were amended with Danish Underground Consortium (DUC) light crude oil to a final

116 concentration of approximately 20 g/kg. To prepare oil contaminated sediment, the

117 sediment was divided into 4 equal portions; one part was thoroughly mixed with oil

118 previously dissolved in hexane. The hexane was evaporated by air-drying the sediment.

119 Finally, the air-dried contaminated sediment was mixed, under nitrogen, with the

120 remaining three parts of the sediment. This procedure has been used in order to achieve

121   a homogenous contamination of the sediment while preserving a large fraction of the

122   sediment microbial communities (Viggi et al., 2015).

123   Microcosms containing oil-supplemented sediment or unamended sediment were

124   prepared in 100-mL glass cylinders. Each cylinder contained (starting from the bottom)

125   ~90 grams of sediment, a layer of Norit® granular activated carbon (10 g, serving as

126   high surface area oxygen reduction catalyst) (Zhang et al., 2009) and 25-30 mL of

127   synthetic brackish medium (Sea Salts, Sigma Aldrich, diluted 1:4). For the "snorkel" and

128   "no oil snorkel" treatments, three graphite rods (the snorkels) were inserted vertically

129   through the layers of different materials to create an electrochemical connection

130   between the anoxic sediment and the oxygenated overlaying water. Replicate

131   microcosms were prepared for each treatment and were sacrificially sampled after

132   incubation for 0, 118, 175, 286 and 466 days.

133   The microcosms were statically incubated in the dark at 20 ± 1 °C. After 0, 118, 175, 286

134   and 466 days of incubation, one cylinder from each treatment was sacrificed,

135   hydrocarbons were extracted from the sediment and analyzed by GC-MS; the aqueous

136   phase (overlying water) was analyzed by ion chromatography (IC) for quantification of

137   anions and the gas phase (i.e., gas pockets accumulating within the sediment) was

138   analyzed by GC-TCD for quantification of methane.

139

140   *2.2   Analytical methods*

141   Methane in the gas pockets was quantified by gas chromatography (GC). Gas samples

142   (50 μL) were taken form voids in the sediment that occurred in some treatments using a

143   gas-tight syringe (Hamilton, Reno, NV, USA) equipped with an 8-cm long needle. Gas

144   samples were analyzed with a Perkin-Elmer Auto System gas chromatograph [stationary

145   phase: stainless-steel column packed with 60/80 Carboxen™ 1000 molecular sieve

146   (Supelco, USA); carrier gas: N_2 at 20 mL/min; oven temperature: 150 °C; injector

147   temperature: 200 °C; thermal conductivity detector (TCD) temperature: 200 °C].

148   Anions in aqueous phase samples were quantified by ion chromatography (IC). Samples

149   were filtered (0.22 μm pore size) and injected into a Dionex DX-100 system (Dionex

150   Corp., Sunnyvale, CA) ion chromatograph (column: IonPac AS14; eluent: sodium

151   carbonate 3.5 mM / sodium bicarbonate 1.0 mM solution). Quantification of total

152   petroleum hydrocarbons (TPH) in sediment samples was performed by GC-MS. In brief,

153   sediment samples were air dried and extracted with a Dionex ASE 200 (Dionex Corp.,

154   Sunnyvale, CA) using an acetone:hexane (1:1 v/v) mixture at 100 °C and a system

155   pressure of 1500 psi. The solvent extract was evaporated under a stream of nitrogen

156   and re-dissolved in 10 mL of an *n*-heptane containing *n*-dodecane (*n*-C_{12}) and *n*-

157   tetracontane (*n*-C_{40}), each at 10 mg/L, as markers for the GC analysis. To purify the

158   hydrocarbon extract (i.e., remove polar compounds), it was percolated through a solid

159   phase extraction cartridge filled with Florisil® and anhydrous sodium sulfate

160   (Chromabond® Na_2SO_4/Florisil®, 6 mL polypropylene columns, 2g/2g). A sample (1 μL)

161   of the purified hydrocarbon extract was then injected (in pulsed split-less mode) into a

162   GC-MS (Perkin Elmer Clarus 680/600; column: HP-5 MS (Agilent) 30 m, ID 0.25 mm,

163   0.25 μm film thickness; carrier gas: helium at 1 mL/min; injector temperature: 280 °C;

164   oven temperature program: initial Temp 40 °C, 18°C/min to 250°C, 10 °C/min to 280 °C,

165   hold for 17 min; MS-scan 30-600, 2-32 min). The TPH amount was determined by

166   summing the unresolved and resolved components eluted from the GC capillary column

167   between the retention times of *n*-C_{12} and of *n*-C_{40}, using solutions of diesel motor oil and

168   diesel mineral oil in hexane as calibration standards (concentration range 0.15–2 g/L).

169

170   *2.3   Microbial Community Analysis with Next Generation Sequencing*

171 Thirty 16S rRNA amplicon libraries were generated representing communities from the

172 sediment used to prepare the microcosms prior to incubation, which were either treated

173 with oil or left untreated (Time 0). The microbial communities were also characterized

174 in samples from sediments from the snorkel, control, no oil snorkel, and no oil control

175 treatments following 175 and 286 days of incubation (n=3 for all). The microbial

176 community analysis was conducted as follows.

177

178 *2.3.1   DNA extraction*

179 Extractions were performed in triplicate from sediment samples (~400 mg) using a

180 PowerSoil® DNA Isolation Kit (Mo Bio Laboratories Inc., USA) with a ribolyser

181 (FastPrep-24, MP Biomedicals, USA). Procedural blanks were performed to ensure

182 extracts remained contamination-free throughout the extraction procedure. DNA

183 extractions were carried out according to the manufacturer's instructions with the

184 following minor modifications: the ribolyser was used at a speed of 6 m/s for 40 s for

185 homogenisation and cell lysis. DNA extracts were stored at -20°C until further use.

186

187 *2.3.2   PCR amplification 16S rRNA genes and PCR product purification*

188 The variable V4/V5 region of the 16S rRNA gene was amplified using the degenerate

189 primers, 515F (GTG-NCA-GCM-GCC-GCG-GTA-A) and 926R (CCG-YCA-ATT-YMT-TTR-

190 AGT-TT) (Quince *et al.*, 2011). In silico testing of the primer set against the SILVA SSU

191 128 Ref NR database using TestPrime 1.0 (Klindworth *et al.*, 2013) returned values of

192 88.2%, 85.8% and 85.7% coverage against the Bacteria, Archaea and Eukarya domains

193 respectively. DNA extracts were diluted (1/10) to reduce the levels of inhibitory

194 contaminants to prevent PCR inhibition (Head, 1999). PCR reactions contained NH_4

195 buffer (50mM), 0.5 mM dNTPs (Invitrogen), 500 nM each primer (ThermoScientific), 2.5

196   U of *Taq* polymerase (Bioline), and 1 μl template DNA in a 20-μl volume. PCR conditions

197   were initial denaturation (94°C, 4 min) followed by 30 cycles (95°C, 1 min; 55°C, 0.45

198   min; 72°C, 1 min) and a final extension (72°C, 10 min) in a thermal cycler (Techne TC-

199   512, Bibby Scientific Limited). PCR products were analyzed by gel electrophoresis with

200   1% (w/v) agarose gel in 1 x TAE buffer (Tris-acetate-EDTA buffer; 40 mM Tris, 20 mM

201   acetic acid, 1 mM EDTA, pH 8.3). Electrophoresis was performed at 100 V for 45 min.

202   Gels were stained with ethidium bromide and visualized with a BioSpectrum Imaging

203   System with VisionWorks LS software (UVP, Cambridge, UK). PCR products were

204   purified with Agencourt AMPure XP PCR purification kit (Beckman Coulter).

205

206   *2.3.3   DNA quantification and Ion Torrent DNA sequencing*

207   Purified DNA was quantified on a Qubit 2.0 Fluorometer (Invitrogen) with a Qubit

208   dsDNA high sensitivity assay kit (Invitrogen). The final concentration of DNA was

209   adjusted to 100 pM, and equimolar concentrations of DNA from all samples were pooled.

210   The pooled amplicon library was sequenced on an Ion Torrent Personal Genome

211   Machine (Life Technologies). Briefly, the library was diluted (26 pM) and emulsion PCR

212   performed on a OneTouch2 instrument with an Ion PGM Template OT2 400 kit

213   according to the manufacturer's instructions (Life Technologies). Beads with bound

214   template DNA were purified on a OneTouch ES system (Life Technologies). Following

215   enrichment, the beads were loaded onto a PGM 316 chip and sequenced in accordance

216   with the manufacturer's instructions.

217

218   *2.3.4   Data analysis*

219   Raw sequence reads were retrieved using the Torrent Suite Software V4.0 (Life

220   Technologies). Sequence reads with a modal length of 428 bp were analyzed in QIIME

221 (Caporaso *et al.*, 2010a). Sequences were assigned to samples based on their unique

222 barcodes and simultaneously filtered to remove reads with no corresponding barcode,

223 reads without the correct primer sequence and poor quality reads (those with a quality

224 value of < 20 were discarded). Operational taxonomic unit (OTU) classifications were

225 performed using UClust (Edgar, 2010), with an OTU threshold defined at 97% sequence

226 identity. OTUs were first clustered open reference against the Greengenes 16S rRNA

227 core alignment (DeSantis *et al.*, 2006) and then clustered de novo. Taxonomy was

228 assigned using RDP Classifier (Wang *et al.*, 2007) and sequences aligned using PyNAST

229 (Caporaso *et al.*, 2010b). Chimeric sequences were identified with ChimeraSlayer (Haas

230 *et al.*, 2011) and removed before subsequent analysis. The average number of reads in

231 individual binned libraries after filtering was 25,868 with a range from 11,214 to

232 139,159 reads. Libraries were rarefied to 11,214 reads for comparative analysis. Core

233 diversity analysis was subsequently performed in QIIME v1.8 to provide a comparative

234 analysis of the microbial communities between samples. BIOM table data, consisting of

235 OTU counts per sample, were imported into Microsoft Excel to determine the average

236 percentage relative abundance (n=3 for all treatments, except T0 where n=6). Phylum

237 and class level comparisons were performed at a level of ≥ 0.2% relative abundance.

238 Abundant taxa for further investigation were determined as those sequences with ≥1%

239 relative abundance. The six amplicon libraries generated from the initial sediments

240 (Time 0) with and without oil were very similar (Pearson correlation at the genus level

241 $R^2 \geq 0.957$, $p \leq 0.01$), these were therefore treated as replicate samples giving n=6 for

242 the Time 0 samples. Sequences have been deposited in the NCBI's Short Read Archive

243 (SRA) under BioProject PRJNA376663.

244

2.4   Catalyzed Reporter Deposition-Fluorescence In Situ Hybridization (CARD-FISH)

analysis

Sediment samples and biofilms growing on the surface of the graphite rods (i.e., the snorkels) were taken for CARD-FISH analysis of the microbial communities. In brief, approximately 1 g of sediment was fixed in formaldehyde (2% v/v final concentration) and cells were extracted from sediment particles as described previously (Barra Caracciolo et al., 2005). The detached cells were filtered through 0.2 μm polycarbonate filters (Ø 47 mm, Millipore) by gentle vacuum (<0.2 bar) and stored at –20°C until use. To remove the biomass from the biofilm formed on the graphite rods, the surface of the electrode was gently scraped with a sterile spatula. The detached biomass was collected in PBS buffer containing 2% v/v formaldehyde, and filtered as described above. CARD-FISH was carried out following a previously published protocol using probes targeting total *Bacteria* (EUB338 I,II,III), and *Deltaproteobacteria* (DELTA495a,b,c) (Fazi et al., 2008).

Probes, labeled with horseradish peroxidase (HRP), were purchased from BIOMERS (http://www.biomers.net). Probe sequences and hybridization conditions were as reported in probeBase (http://www.microbial-ecology.net/probebase). DAPI (4′,6-diamidino-2-phenylindole) staining was performed to determine total cell numbers, from which the relative abundances of each targeted bacterial population was calculated. Total cell counts were performed at the end of the CARD-FISH hybridization procedure by mounting the samples in Vectashield Mounting Medium with DAPI (Vector Labs, Italy). At least 20 randomly selected microscopic fields for each sample were analyzed to enumerate the cells by microscopic analysis. Slides were examined by epifluorescence microscopy (Olympus, BX51) and the images were captured with an

269   Olympus F-View CCD camera and images were processed with CellˆF software

270   (Olympus, Germany).

271

272   *2.5   geneCARD-FISH assay*

273   GeneCARD-FISH assays were conducted on small sections of filter (see section 2.3)

274   according to a previously described protocol (Matturro et al., 2016), as detailed in the

275   following paragraphs.

276

277   *2.5.1   Polynucleotide probe design and synthesis*

278   Polynucleotide probes targeting the gene encoding the alpha subunit of alkylsuccinate

279   synthase (*assA*) were synthesized using a PCR DIG Probe Synthesis Kit (Roche, Italy)

280   following the manufacturer's instructions. A cloned *assA* gene, obtained from a

281   hydrocarbon-degrading sulfate-reducing enrichment culture (Aitken et al., 2013), was

282   used as DNA template. Primers assA2F and assA2R (Aitken et al., 2013) were used for

283   PCR amplification. PCR Dig-labeled amplicons were purified with QIAquick PCR

284   Purification Kit (Qiagen, Italy) and run on a 2% agarose gel to check the incorporation of

285   DIG molecules. The concentration of purified DIG-labeled polynucleotide probe was

286   quantified (NanoDrop ND-2000, Italy) and aliquots (10 ng/μL) were stored at - 20°C and

287   employed during the hybridization step of the geneCARD-FISH assay.

288

289   *2.5.2   Hybridization*

290   Before hybridization, cells were pretreated with lysozyme and proteinase K as

291   previously described (Matturro et al., 2016). Filters were transferred to 100 μL of pre-

292   hybridization buffer HB-I containing the following compounds: 0.25 mg/mL of thymus

293   DNA, yeast RNA 0.25 mg/mL, formamide 50%, Saline Sodium Citrate SCC 5X, dextran

294   sulfate 10%, SDS 0.1%, EDTA 20 mM, blocking reagent 1% (molecular biology reagents,

295   Sigma Aldrich, Italy) and incubated at 46°C for 1.5 h. Filters were then transferred to a

296   fresh tube containing 100 μL of HB-I and DIG-labeled polynucleotide probe (final

297   concentration 0.5 ng/μL) and then incubated in a thermocycler with the following

298   cycles: 70°C for 25 min (DNA denaturation) and 46°C overnight (Dig-labeled probe

299   hybridization). After hybridization, filters were immersed in washing buffer WB-I (SSC

300   10X, SDS 0.1%) for 30 min at 48°C and then transferred into washing buffer WB-II (SSC

301   0.1X, SDS 0.1%) for 90 min at 48°C.

302

303   *2.5.3   Immunochemical probe detection*

304   Filters were incubated in an antibody buffer AB-I for 45 min at room temperature.

305   Buffer AB-I consisted of a Western Blocking reagent solution 1% (Sigma Aldrich, Italy)

306   in phosphate buffered saline, 1X PBS (145 mM NaCl, 1.4 mM NaH_2PO_4, 8 mM Na_2HPO_4,

307   pH 7.4).   Filters were then immersed into an AB-I buffer solution containing the

308   antibody anti-DIG (Anti-Digoxigenin-POD Fab fragments, Sigma Aldrich, Italy) to a final

309   concentration of 0.3U/mL for 90 min at room temperature. After incubation, filters were

310   washed for 10 min in fresh AB-I buffer at room temperature. Filters were then washed

311   10X PBS solution for 20 min at room temperature.

312

313   *2.5.4   Fluorescent signal amplification*

314   After the immunochemical reaction, filters were placed in the substrate mix with dye-

315   tyramide for 15 min at 37°C and then washed in 1X PBS for 30 minutes at room

316   temperature, in water for 1 min and finally in 96% ethanol for 1 min. The filters were

317   air-dried, placed on a microscope slide and stained with DAPI (4,6-diamidino-2-

318   phenylindole) to determine total cell numbers in the samples.

319

2.5.5   Microscopy analysis

Hybridized cells carrying the *assA* gene were visualized by epifluorescence microscopy

(Olympus, BX51) and quantified by counting fluorescent cells (at least 100 cells per

grid) on random grids on filter sections. Quantitative data were expressed as cell

numbers per g dry weight of sediment.

2.6   X-Ray Photoelectron Spectroscopy of graphite electrodes

The surface chemical composition of the graphite rods was determined by using X-ray

photoelectron spectroscopy (XPS). XPS measurements were performed in a VG Escalab

MkII spectrometer (VG Scientific Ltd, East Grinstead, UK) with a 5-channeltron detection

system and an unmonochromatized radiation source of Al Kα (1486.6 eV). The

electrostatic lenses were operated in the selected-area mode A3x12, providing

photoelectron collection from the sample area with a diameter of about 3 mm. The

binding energy (BE) scale was calibrated by using the C1s peak of graphite at BE = 284.6

eV. All the spectra were acquired at the pass energy of 50 eV. Spectroscopic data were

processed using Avantage v.5 software, using a peak-fitting routine with Shirley

background and Scofield sensitivity factors for elemental quantification.

## 3.   Results and discussion

3.1   Sulfate reduction

Sulfate is one the most abundant electron acceptors in anoxic marine and brackish

sediments and typically plays a critical role in the oxidation of organic matter in pristine

and contaminated sediments. Sulfate concentration in the snorkel treatments and

344 control microcosms was monitored following incubation for 0, 118, 175, 286, and 466

345 days (Figure 1). In the oil-supplemented control with no snorkel ("control"), sulfate

346 concentration remained nearly constant during the initial 118 days of incubation

347 (Figure 1); thereafter, sulfate gradually decreased over time and was almost completely

348 depleted by day 466 (Figure 1). By contrast, significantly greater initial sulfate reduction

349 rates were observed in the oil-supplemented snorkel-containing sediments (two-tailed

350 t-test, p<0.005), with over 85% of the initial sulfate (i.e., approximately 1,000 mg/L)

351 consumed by day 118 (Figure 1). Notably, sulfate reduction was observed also in

352 microcosms that were not supplemented with oil, being most likely fuelled by the

353 indigenous organic carbon in the River Tyne sediment. Also in this case, the snorkel

354 accelerated (though to a lower extent) the removal of sulfate, with no-oil snorkel

355 treatments displaying a 35% greater cumulative sulfate removal compared to the no-oil

356 controls by day 118 (p=0.06), and a 25% greater cumulative removal by day 286

357 (p=0.005) (Figure 1). Notably, by comparing sulfate concentrations in the control and in

358 the no oil control experiments, it is apparent that, in the absence of the snorkel, the

359 presence of oil slightly inhibited the activity of sulfate reducing microorganisms in the

360 River Tyne sediments (Figure 1).

361 A recent study (Daghio et al., 2016), suggested that an electrode potentiostatically

362 poised at an oxidative value of +300 mV vs. SHE, was capable of indirectly stimulating

363 the sulfate-driven anaerobic oxidation of toluene, through the electrochemical

364 scavenging of hydrogen sulfide, a toxic end product of dissimilatory sulfate reduction

365 (Reis et al., 1992). This hypothesis was supported by the accumulation of elemental

366 sulfur on the surface of the poised carbon-based electrode.

367
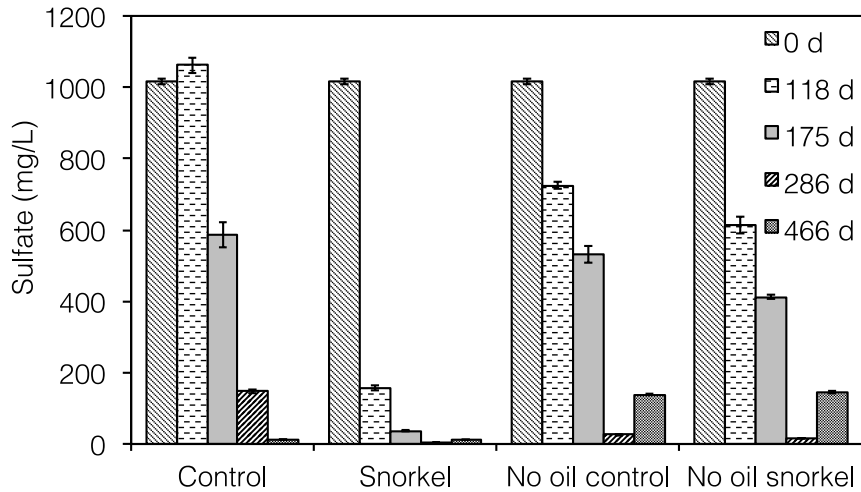
Figure 1. Concentration of sulfate in the snorkel experiments and controls throughout

the experimental period. Error bars represent the standard error of replicate samples.

370

371

3.2   XPS analysis of graphite electrodes

To test the assumption that the enhancement of sulfate reduction may be due to the

electrochemical scavenging of sulfide, at the end of the study (day 466), the surface of

the graphite rods (from the snorkel and the no oil snorkel treatments) were analyzed via

XPS. For comparative purposes, an identical pristine graphite rod was also analyzed.

Interestingly, XPS analyses did not reveal the presence of elemental sulfur in any of the

snorkel treatments. However, substantial amounts of oxidized iron species, namely

$Fe_2(SO_4)_3$ and Fe_2O_3, were detected on the surface of the snorkels (Figure 2). Notably,

when the rods were extracted from the sediments, prior to being analyzed by XPS

analysis, they appeared to be covered by reddish precipitates, providing a further

qualitative indication of the occurrence of oxidized iron species.

Importantly, the abundance of Fe^{3+} species in the oil-supplemented snorkel (2.8 atomic

%) was 4-fold higher than in the no-oil snorkel (0.7 atom%) (Figure 2), raising the

385 intriguing possibility that the accumulation of iron precipitates was correlated with the

386 rate and extent of observed sulfate reduction. Accumulation of oxidized iron species on

387 the surface of a conductive snorkel deployed in crude oil marine sediment was also

388 observed in a previous oil-spill snorkel experiment (Viggi et al., 2015).
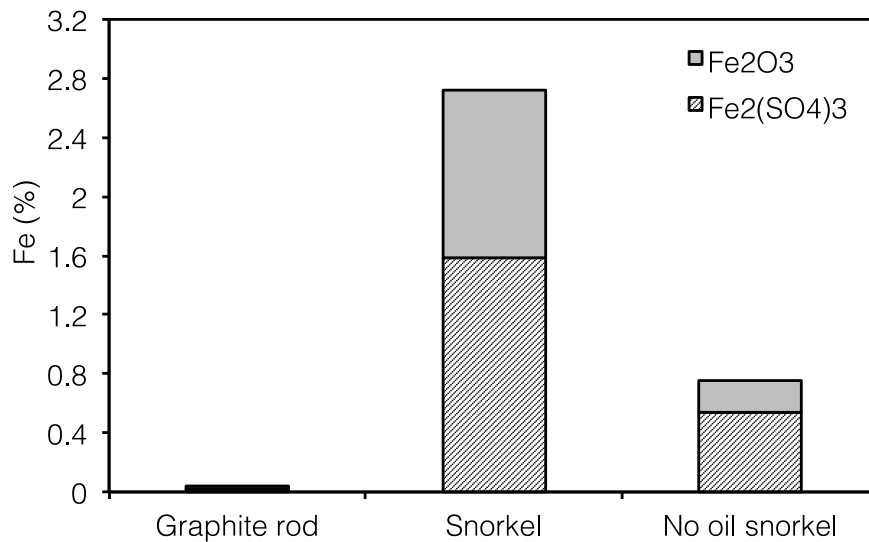
389

390 **Figure 2.** Percentage of Fe species on the surface of oil-supplemented and no oil snorkel

391 experiments, and in untreated graphite rods.

392

393

394 *3.3   Gas production*

395 The presence of snorkels markedly affected gas production and methanogenic activity in

396 River Tyne sediments. Indeed, gas pockets containing methane (up to 25% vol/vol)

397 accumulated within the sediment in control microcosms, which did not contain the

398 snorkel (Figure 3). By contrast, negligible gas production occurred in oil-supplemented

399 and no-oil snorkel treatments. Although the total cumulative volume of gas produced in

400 each treatment could not be precisely determined, the higher percentage of methane

401 observed on days 118 and 175 in the gas pockets occurring in oil-supplemented controls

402   relative to the no-oil controls, provides an indication that at least some of the produced

403   methane might derive from degradation of oil constituents, with the remainder likely

404   deriving from the degradation of the organic matter already present in the sediment. In

405   fact, methanogenic crude oil-degrading capacity has already been reported in the River

406   Tyne sediments (Gray et al., 2011; Jones et al., 2008). In both oil-supplemented and no-

407   oil controls, gas production peaked on day 118 and became nearly undetectable by day

408   286 (Figure 3).
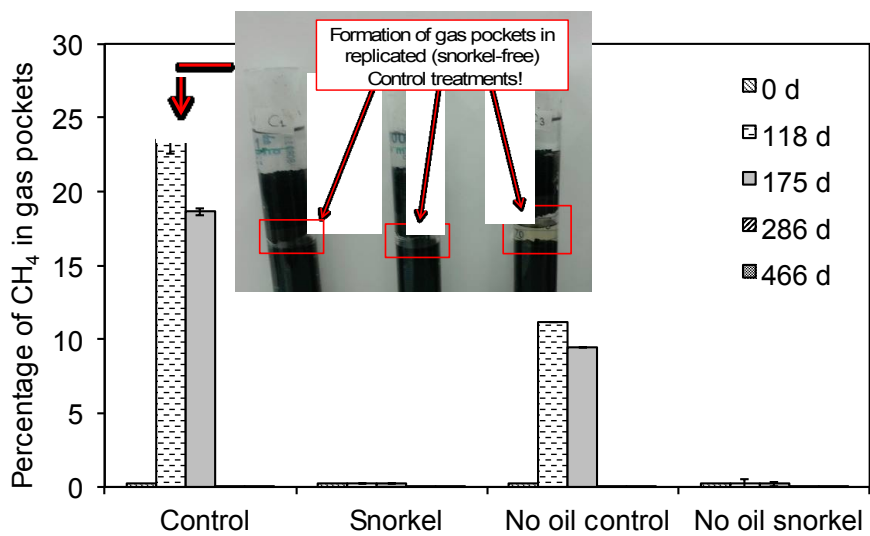
409

410   **Figure 3.** Percentage (%, vol/vol) of methane in gas pockets formed in snorkel-free

411   control experiments. Error bars represent the standard error of replicate samples. The

412   inset photo illustrates the gas pockets seen in snorkel-free sediments.

413

414

415

416   A large number of studies focusing on the anaerobic decomposition of organic matter in

417   both freshwater and marine environments have stressed the importance of sulfate

418   reduction and methanogenesis (Kuivila et al., 1989; Lovley and Klug, 1986; Oremland

419   and Polcin, 1982; Oremland and Taylor, 1978). Thermodynamic and kinetic reasoning

420   suggests that sulfate-reducing bacteria can outcompete methanogens due to the higher

421   energy yield of sulfate reduction to sulfide driven by H_2 (or acetate) relative to the

422   corresponding reduction of carbon dioxide to methane (or acetate disproportionation to

423   methane and carbon dioxide), as well as to the higher growth rate of sulfate reducers on

424   these substrates, compared to methanogens (Conrad et al., 1986). Here, in microcosms

425   containing the snorkel, sulfate-reducing bacteria almost completely outcompeted

426   methanogens. By contrast, in microcosms not containing the snorkel, sulfate reduction

427   (though at lower rate than in the snorkel experiments) and methanogenesis occurred

428   simultaneously, suggesting the two metabolic processes are competitive yet not

429   mutually exclusive (Paulo et al., 2015).

430

431   *3.4   Crude oil biodegradation*

432   In oil-supplemented microcosms, the removal of TPH appeared to be accelerated (up to

433   30% greater removal by day 175, $p<0.05$) by the presence of the snorkel (Figure 4).

434   These findings are consistent with the results of a previous microcosm study carried out

435   using a different sediment contaminated with a different oil, hence indicating that the

436   snorkel-induced stimulatory effect on hydrocarbon biodegradation was reproducible in

437   sediments from distant geographical locations (Viggi et al., 2015).

438   Consistent with the industrial setting from which the River Tyne sediments were

439   obtained, low levels of hydrocarbons were detected in the microcosms, which were not

440   specifically amended with the DUC crude oil (Figure 4). In these microcosms, TPH

441   concentration decreased over time to a similar extent both in the no oil control and in

442   the no oil snorkel treatments. No stimulatory effect of the snorkel on removal of

443   indigenous hydrocarbon contamination was apparent, possibly due to the fact that the

444   indigenous hydrocarbons in the River Tyne sediment resulted from chronic

445   contamination and were probably less available to the hydrocarbon-degrading

446   organisms present, compared to freshly spiked hydrocarbons in the oil-supplemented

447   treatments.
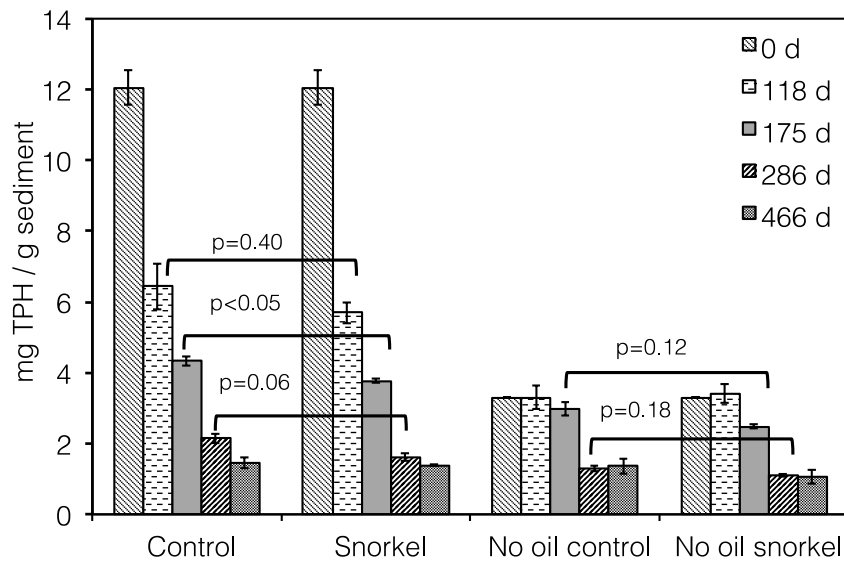
448

449   **Figure 4.** Concentration of TPH in the different in snorkel experiments and controls

450   throughout the experimental period. Error bars represent the standard error of

451   replicate samples.

452

453

454   *3.5   Effect of electrochemical snorkels on sediment microbial communities*

455   Thirty 16S rRNA gene amplicon libraries were generated which represented microbial

456   communities from the bulk sediment at the start of the experiment (T0) and in the

457   snorkel, no oil snorkel, control, and no oil control treatments following 175 and 286

458   days of incubation (Figure 5). The microbial composition across the 30 amplicon

459   libraries was 98.6% ±0.61 Bacteria (range 97.8-99.5) and 1.4% ±0.61 Archaea (range

460   0.5-2.2). At the phylum level, archaeal sequences comprised a small percentage of the

461   total microbial communities (*Euryarchaeota* 0.3% ±0.10; *Crenarcheota* 0.6% ±0.17

462   relative abundance, Figure 5), and therefore archaeal communities were not

investigated further. The most abundant phyla in the snorkel treatment at 175 days

were *Chloroflexi* (21%), *Bacteriodetes* (20%), *Tenericutes* (15%), *Firmicutes* (13%),

Deltaproteobacteria (5%), OP9 (4%), *Alphaproteobacteria*, *Actinobacteria* and

Gammaproteobacteria (3%), and *Betaproteobacteria*, *Synergistetes* and *Planctomycetes*

(1%) (Figure 5, Supplemental Figure S1A). Successional changes in the microbial

communities in the snorkel treatment were detected by day 286 with a decrease in the

relative abundance of *Tenericutes* (from 15% to 0.3%), and an increase in OP9 (from 4%

to 16%) and *Gammaproteobacteria* (from 3% to 26%) (Figure 5, Supplemental Figure

S1B). *Deltaproteobacteria* were detected in high relative abundance in the initial

sediments (T0, 22%), with a subsequent decrease in abundance in all treatments (Figure

5).
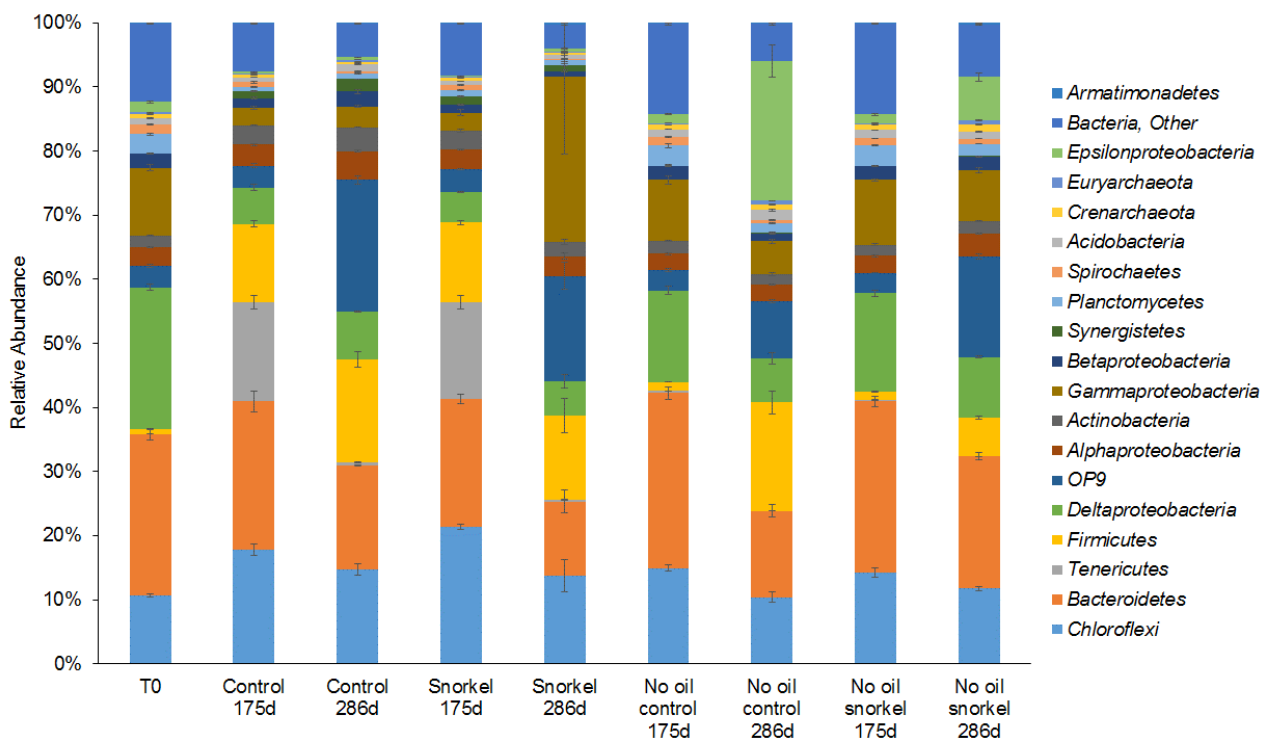
Figure 5. Phylum level comparison of microbial communities in River Tyne oil spill
snorkel experiments. The phylum Proteobacteria were further sub-divided into Class.

478 Error bars represent the standard error of replicate samples (n=3, except T0 where

479 n=6).

480

481 *3.5.1 Putative n-alkane degraders*

482 At a higher resolution within the *Chloroflexi*, the uncultured genera T78 and SHD-231 in

483 the order *Anaerolineales* were enriched at 175 and 286 days in the snorkel and control

484 experiments which contained oil, compared to the controls without oil and the initial

485 sediments (Figure 6A, Supplemental Figure S2). A significant enrichment of the

486 *Anaerolinea*, predominantly in the oil-amended treatments, suggests a role in crude oil

487 biodegradation within the sediments. The obligately anaerobic, non-photosynthetic

488 *Anaerolinea* (Yamada et al., 2006) have previously been implicated in oil biodegradation

489 coupled to sulfate-reduction in River Tyne sediment microcosms (Sherry et al., 2013a),

490 in methanogenic oil sands tailings ponds (An et al., 2013), in enrichments cultures from

491 a low-temperature, sulfidic natural hydrocarbon seep (Savage et al., 2010) and in oil

492 contaminated mud-flat sediments (Sanni et al., 2015). Specifically, the uncultured genus

493 T78 have been described as saccharolytic (Yamada et al., 2006) and carbohydrate

494 utilisers (Miura and Okabe, 2008; Yamada and Sekiguchi, 2009). T78 have been

495 identified in samples from four biogas plants and six wastewater treatment plants used

496 as inocula to investigate the degradation of cellulose and straw in batch cultivation tests

497 (Sun et al., 2016). T78 have also been detected in anaerobic digesters processing sewage

498 sludge (Ariesyady et al., 2007) and used for co-digestion of whey permeate and cow

499 manure (Hagen et al., 2014). The increasing occurrence of the prescence of members of

500 the *Anaerolineae* in this study and previous studies suggests they may play a key role in

501 anaerobic hydrocarbon degradation.

502   Organisms from the *Tenericutes* from within the Class *Mollicutes* were significantly

503   enriched in oil-amended snorkel and control experiments at 175 days, compared to the

504   oil-free controls and initial sediments (Figure 6B). The apparent absence of *Mollicutes* in

505   the initial sediments (Time 0), the significant enrichment in only those experiments

506   which contain oil at 175 days (where ~4 mg TPH/g sediment remained in both systems)

507   and the absence of *Mollicutes* in the oil-free controls suggests members of the *Mollicutes*

508   play a role in the degradation of crude oil compounds. *Mollicutes* have previously been

509   detected in salt-marsh sediment microcosms treated with Mississippi Canyon Block 252

510   oil (MC252) from the Deepwater Horizon (DH) spill, where they were described as 'late

511   responders' to the oil as their relative abundance did not increase until 3 weeks after the

512   addition of the oil (Hagen et al., 2014). In another Deepwater Horizon study, *Mollicutes*

513   were found in the gut of oysters taken from oil-contaminated areas (King et al., 2012),

514   suggesting a tolerance of members of the *Molllicutes* to hydrocarbons. *Tenericutes*

515   (*Mollicutes*) have also been found as important components of the microbial

516   communities associated with natural hydrocarbon seeps (Skennerton et al., 2016).

517

518   *3.5.2   Sulfate-reducing bacteria (SRB) and fermentative Clostridia*

519   The relative abundance of *Deltaproteobacteria* was highest in the time 0 sediments

520   (22% of reads from *Deltaproteobacteria*; Figure 6C), when sulfate concentration was

521   high ~1000mg/L. By day 175 reads from *Deltaproteobacteria* decreased to around 5%

522   relative abundance in both treatments containing oil (control and snorkel; Figure 6C)

523   despite differences in the levels of sulfate at this time point (control ~ 600 mg/L,

524   snorkel ~ 10 mg/L). In treatments without oil addition the relative abundance of reads

525   from *Deltaproteobacteria* was greater than 14-15%; Figure 6C). This suggests that some

526   deltaproteobacterial SRB may be sensitive to the addition of oil as has been shown

527   previously (Koo et al., 2015). Moreover, previous studies of sulfate-driven oil

528   degradation in River Tyne sediments have indicated that despite oil degradation clearly

529   being driven by sulfate-reduction, selection for deltaproteobacterial sulfate-reducing

530   bacteria was modest (Sherry et al., 2013a). It has been suggested that this may be due to

531   petroleum hydrocarbon degradation in these systems being driven by sulfate-reducers

532   acting as terminal oxidizers in a syntrophic food chain, rather than being the primary

533   hydrocarbon oxidizers, and thermodynamic arguments have been proposed in support

534   of this hypothesis (Head et al., 2014). Further evidence to support the possibility that

535   sulfate-reducers are terminal oxidizers in a syntrophic food chain is the enrichment of

536   organisms from the class *Clostridia* within the *Firmicutes* on day 175 and 286 in both oil-

537   amended treatments (control and snorkel ~10% of reads, Figure 6D) relative to the oil-

538   free controls and the sediments at time 0 (0.6-4% of reads, Figure 6D). Within the

539   *Clostridiales*, the genera *Fusibacter* and *Dethiosulfatibacter* were enriched in response to

540   oil on day 175 and 286 (control and snorkel, Figure 6E and 6F) compared to oil-free

541   controls and the sediments at time 0. *Fusibacter* spp. have been associated with oil-

542   producing wells (Ravot et al., 1999), sites contaminated with chlorinated solvents (Lee

543   et al., 2011), and degradation of PAHs following the Deepwater Horizon spill (Kappell et

544   al., 2014). Furthermore, *Fusibacter* were shown to be involved in the degradation of

545   alkanes, crude oil and aromatics to volatile fatty acids (VFAs) in a study investigating

546   which crude oil components contribute to oil field souring (Hasegawa et al., 2014).

547   *Fusibacter* prefer anaerobic environments and are thiosulfate-reducers with a

548   fermentative metabolism that can produce acetate, butyric acid, CO_2, and H_2 from

549   carbohydrates (Basso et al., 2009). Similarly, *Dethiosulfatibacter* are able to use

550   thiosulfate and elemental sulfur as electron acceptors and can produce CO_2, H_2, acetate,

551   and propionate from organic matter (Takii et al., 2007). Interestingly, geochemical data

552   suggest that in the presence of crude oil, the snorkel may promote oxidation of sulfide to

553   elemental sulfur and/or thiosulfate, potentially explaining the selection of these

554   organisms in treatments containing electrochemical snorkels (see section 3.7 below).

555   Both *Fusibacter* and *Dethiosulfatibacter* are hydrogen-producing acetogenic bacteria

556   that are potentially involved in fermenting components of oil to VFA which may be

557   utilized by sulfate-reducing terminal oxidizers.

558
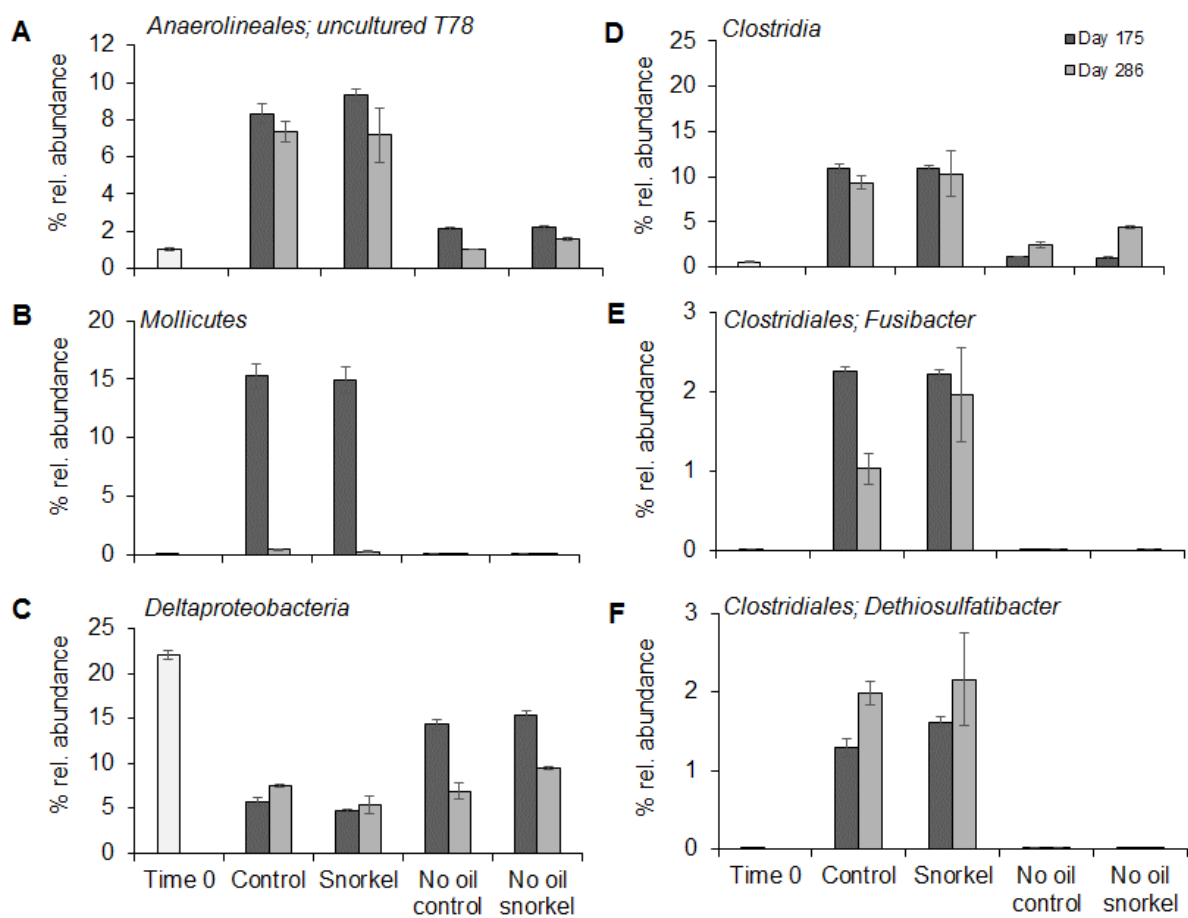
559

560   **Figure 6.** Relative abundance (%) of rRNA gene sequences (n=11214) from oil spill

561   snorkel experiments at 0, 175 and 286 days. The uncultured genus T78 lineage in the

562   order *Anaerolineales* (A), class *Mollicutes* (B), class *Deltaproteobacteria* (C), class

563   *Clostridia* (D), genus *Fusibacter* (order *Clostridiales*) (E) and genus *Dethiosulfatibacter*

564   (order *Clostridiales*) (F). Error bars denote standard error (n=3, except Time 0 where

565   n=6). Note differences in scale.

566

567

568   *3.6   Effect of electrochemical snorkels on abundance of prokaryote cells,*

569   *Deltaproteobacteria and anaerobic alkane-degrading bacteria*

570   Consistent with the effect of electrochemical snorkels on sulfate-reduction rates and

571   hydrocarbon degradation, the snorkel and the supplied oil were found to exert an effect

572   on the overall abundance of prokaryote cells. After 286 days of incubation, in the oil-

573   supplemented snorkel treatment, the abundance of DAPI-stained cells in the bulk

574   sediment was higher (p=0.007) than in the corresponding control ($4.4\pm0.1 \times10^8$ vs.

575    $2.9\pm0.1 \times10^8$ cells per gram of dry sediment; Figure 7a). This corroborated the

576   suggestion that electrochemical snorkels promoted growth-linked metabolism within

577   the oil-treated sediment (Figure 7a). Notably, the DAPI cell counts in the bulk sediment

578   of no-oil controls ($3.9\pm0.1 \times10^8$ cells per gram of dry sediment) was substantially higher

579   than in the oil-supplemented controls with no snorkel, clearly indicating that the

580   presence of oil adversely affected microbial activity (Figure 7a).

581   The trend in total cell counts was mirrored by the abundance of *Deltaproteobacteria* in

582   the different treatments. Their higher abundance in the oil-supplemented snorkels with

583   respect to the (oil-supplemented) controls is consistent with the observed positive effect

584   of the snorkel on sulfate-reducing activity and alkane degradation. The trend in the

585   *Deltaproteobacteria* was also mirrored in the relative abundance data at 286 days (cf.

586   Figure 7b with Figure 6C).

587   An increasing number of studies have shown that fumarate addition is a key mechanism

588   of alkane activation under anoxic conditions (Callaghan et al., 2010; von Netzer et al.,

26

589   2013). This reaction is catalyzed by alkylsuccinate synthase. The gene encoding the

590   alpha subunit of alkylsuccinate synthase *assA*, can serve as a biomarker of anaerobic

591   alkane degradation. Here, a geneCARD-FISH approach was employed to enumerate the

592   presence and enrichment of cells carrying the *assA* gene in the different treatments, both

593   in the bulk sediment and on the surface of the graphite snorkels. Interestingly, after 286

594   days of incubation, the measured concentration of cells carrying the *assA* gene was

595   similar to the abundance of *Deltaproteobacteria*, suggesting that sulfate-reducing

596   bacteria also played a role in direct petroleum hydrocarbon oxidation in River Tyne

597   sediments (Sherry et al., 2013b). It remains unclear why, in no-oil treatments, the

598   measured concentration of *Deltaproteobacteria* and cells carrying the *assA* gene was

599   higher than in the oil-supplemented microcosms. This may result from the fact, that in

600   the absence of snorkels the presence of oil adversely affected the autochthonous

601   microbial populations in the sediment, as is evident from the DAPI count data and the

602   Ion Torrent sequencing data (Figure 6C and 7A). Analysis of the biofilm growing on the

603   surface of the snorkels indicated that cells carrying the *assA* gene were present at

604   comparable levels (11±2 vs. 7±1 % of total bacteria) in the oil-supplemented snorkels

605   and the no-oil snorkels, suggesting a minor role for the electrode biofilm in the observed

606   degradation of hydrocarbons.

607
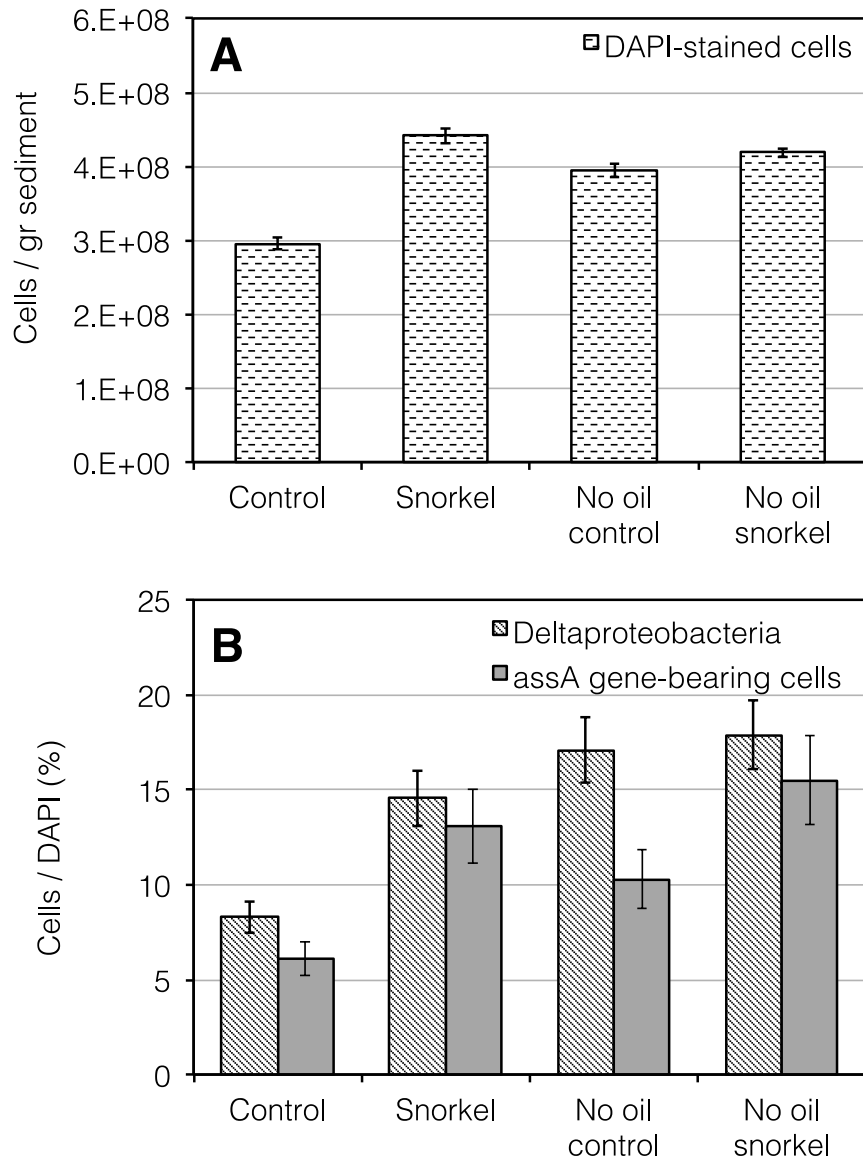
Figure 7. Concentration of total DAPI-stained cells in the bulk sediment of the different

experiments (a). Concentration of *Deltaproteobacteria* (as detected by CARD-FISH) and

of cells carrying the *assA* gene in the bulk sediment of the different treatments (as

detected by geneCARD-FISH) (b). All measurements were carried out on samples taken

after 286 days of incubations. Error bars represent the standard error of replicate

samples.

614

615

616 *3.7   Interaction of graphite electrodes and sediment biogeochemical cycles*

617   This study provides evidence that bridging spatially separated redox zones (i.e., the

618   anoxic sediment with the oxic overlying water) with an electrically conductive snorkel

619   has a remarkable impact on a number of biogeochemical processes taking place in the

620   bulk sediment, even at a substantial distance from the surface of the conductive element

621   (i.e., the snorkel). The most striking finding was the acceleration of sulfate reduction in

622   the presence of an electrochemical "snorkel", with this process being apparently coupled

623   to the formation of oxidized iron species on the surface of the snorkel. Possibly, Fe(III)

624   species accumulating at the surface of the rod derived from the reductive dissolution of

625   iron minerals (e.g., Fe(III) (hydr)oxides) in the sediment into Fe(II), driven by

626   biogenically produced hydrogen sulfide (Aller and Rude, 1988), followed by the

627   (bio)electrochemical re-oxidation of Fe(II) to Fe(III) at the electrode surface (Figure 8).

628   It is worth noting, that GC-MS analyses of sediment extracts indicated the presence of

629   substantial amounts of elemental sulfur in the River Tyne sediments (data not shown),

630   suggesting that this compound was a likely product of hydrogen sulfide oxidation, and

631   that this reaction most probably also occurred under "natural" conditions. Interestingly,

632   thermodynamic calculations indicated that sulfide oxidation to elemental sulfur coupled

633   to Fe(III) reduction to Fe(II), under conditions relevant to those occurring in the snorkel

634   experiments (i.e., pH, concentration of reactants and products), is extremely sensitive to

635   Fe(II) concentration and becomes endergonic at Fe(II) concentrations higher than 10^{-5}

636   M (Figure 9). This provides an indication that, by scavenging Fe(II), the snorkel may

637   affect hydrogen sulfide accumulation and in turn sulfate reduction.

638

639
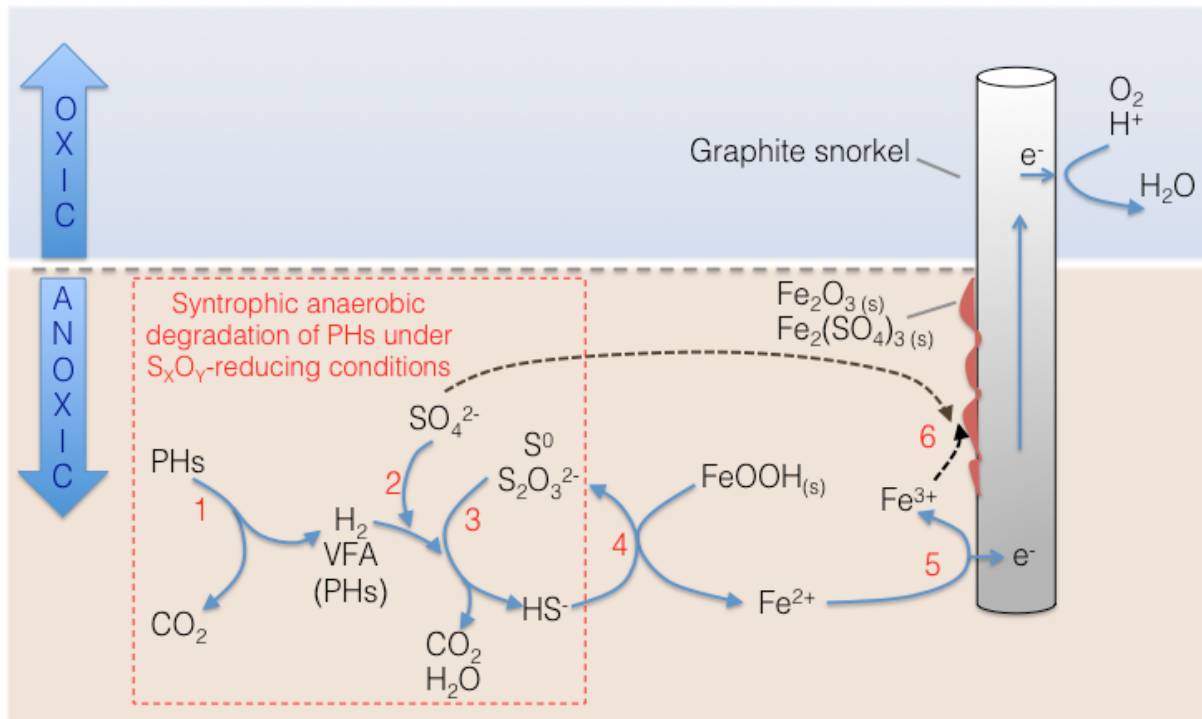
Figure 8. Tentative model depicting the effects of an electrochemical snorkel on

chemical and biological reactions taking place in sediments contaminated by petroleum

hydrocarbons. Legend: (1) Fermentative degradation of Petroleum Hydrocarbons (PHs),

tentatively catalyzed by *Clostridia*; (2) Sulfate reduction coupled to oxidation of

fermentation products or petroleum hydrocarbons, tentatively catalyzed by

Deltaproteobacteria; (3) Sulfur / thiosulfate reduction coupled to oxidation of

fermentation products; (4) Abiotic reduction of Fe(III)hydroxides coupled to oxidation

of sulfide to sulfur / thiosulfate; (5) Biotic/abiotic oxidation of Fe^{2+} coupled to electrode

reduction; (6) Precipation of poorly soluble Fe(III) compounds.

649

650

651

$$2FeOOH + HS^- + 5H^+ \Longrightarrow 2Fe^{2+} + S^0 + 4H_2O$$
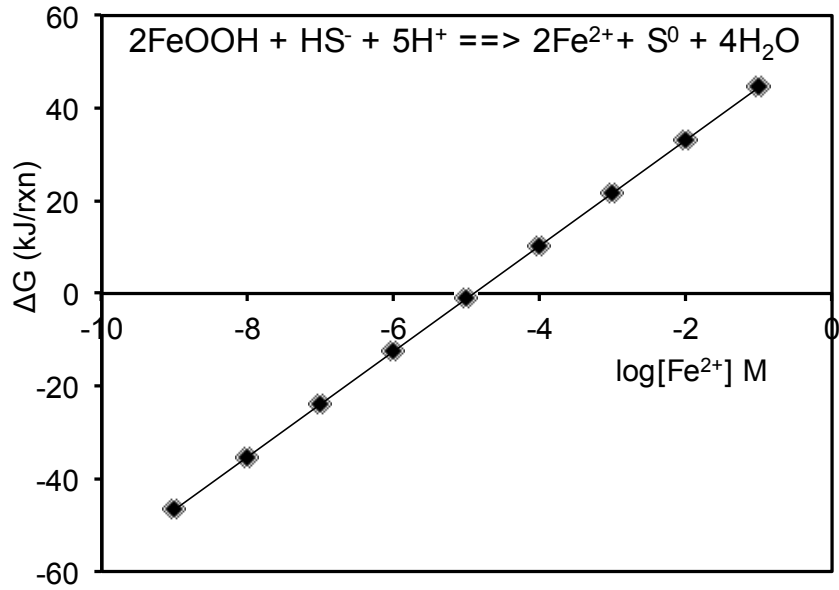
652

653 **Figure 9.** Influence of Fe^{2+} concentration on the Gibbs free energy change of Fe(III)

654 (hydr)oxide reduction by hydrogen sulfide.

655

656

657 **4.   Conclusions**

658 The results of this study provide an additional line of evidence that a microbial

659 electrochemical snorkel (i.e., a single graphite electrode half-buried in anoxic sediments

660 and half exposed to oxygenated overlying water) has a remarkable impact on

661 biogeochemical redox processes taking place in the bulk sediment. The most noticeable

662 effect was observed on sulfate reduction, which was substantially accelerated by the

663 presence of the snorkel compared to snorkel-free controls, while methanogenesis was

664 apparently suppressed. Accumulation of oxidized iron species on the electrode surface,

665 along with thermodynamic calculations suggested that the occurrence of a sulfide-

666 driven iron redox cycle was triggered by the presence of the snorkel. Acceleration of

667 sulfate reduction corresponded to a slightly enhanced removal of petroleum

668 hydrocarbons may be facilitated by removal of toxic sulfide linked to reduction of iron

31

669   oxides in the sediment. This process may enhance overall sulfide oxidation with the

670   Fe(II) generated from sulfide oxidation being removed by oxidation at the

671   snorkel/electrode surface, maintaining a low Fe(II) concentration that provides a

672   thermodynamic driver favoring sulfide oxidation, while replenishing Fe(III) as an

673   oxidant, sustaining the process over extended time periods.

674

675

680

681   **Author contribution**

682   C.C.V. set up and monitored the oil-spill snorkel experiments. B.M., E.F., and S.R.

683   performed and analyzed FISH experiments. S.I. developed the GC-MS method and

684   contributed to the interpretation of chemical data. A.M and S.K performed and analyzed

685   XRD experiments. A.S. and O.K.M. and I.M.H performed NGS analysis. E.V. and K.R.

686   contributed the analysis and interpretation of Fe and S biogeochemical cycles. F.A

687   conceived the experimental plan. All authors contributed to writing of the manuscript.

688   F.A., S.R., K.R. and I.M.H. were co-Investigators on the Kill-Spill Project.

689 **References**

690 Aitken, C.M., Jones, D.M., Maguire, M.J., Gray, N.D., Sherry, A., Bowler, B.F.J., Ditchfield,

691   A.K., Larter, S.R., Head, I.M., 2013. Evidence that crude oil alkane activation

692   proceeds by different mechanisms under sulfate-reducing and methanogenic

693   conditions. Geochim. Cosmochim. Acta 109, 162–174.

694   doi:10.1016/j.gca.2013.01.031

695 Aller, R.C., Rude, P.D., 1988. Complete oxidation of solid phase sulfides by manganese

696   and bacteria in anoxic marine sediments. Geochim. Cosmochim. Acta 52, 751–765.

697   doi:10.1016/0016-7037(88)90335-3

698 An, D., Brown, D., Chatterjee, I., Dong, X., Ramos-Padron, E., Wilson, S., Bordenave, S.,

699   Caffrey, S.M., Gieg, L.M., Sensen, C.W., Voordouw, G., Scherer, S., 2013. Microbial

700   community and potential functional gene diversity involved in anaerobic

701   hydrocarbon degradation and methanogenesis in an oil sands tailings pond 1.

702   Genome 56, 612–618. doi:10.1139/gen-2013-0083

703 Ariesyady, H.D., Ito, T., Okabe, S., 2007. Functional bacterial and archaeal community

704   structures of major trophic groups in a full-scale anaerobic sludge digester. Water

705   Res. 41, 1554–1568. doi:10.1016/j.watres.2006.12.036

706 Bargiela, R., Mapelli, F., Rojo, D., Chouaia, B., Tornés, J., Borin, S., Richter, M., Del Pozo, M.

707   V., Cappello, S., Gertler, C., Genovese, M., Denaro, R., Martínez-Martínez, M.,

708   Fodelianakis, S., Amer, R.A., Bigazzi, D., Han, X., Chen, J., Chernikova, T.N., Golyshina,

709   O. V., Mahjoubi, M., Jaouanil, A., Benzha, F., Magagnini, M., Hussein, E., Al-Horani, F.,

710   Cherif, A., Blaghen, M., Abdel-Fattah, Y.R., Kalogerakis, N., Barbas, C., Malkawi, H.I.,

711   Golyshin, P.N., Yakimov, M.M., Daffonchio, D., Ferrer, M., 2015. Bacterial population

712   and biodegradation potential in chronically crude oil-contaminated marine

713   sediments are strongly linked to temperature. Sci. Rep. 5, 11651.

714   doi:10.1038/srep11651

715 Barra Caracciolo, A., Grenni, P., Cupo, C., Rossetti, S., 2005. In situ analysis of native

716   microbial communities in complex samples with high particulate loads. FEMS

717   Microbiol. Lett. 253, 55–58. doi:10.1016/j.femsle.2005.09.018

718 Basso, O., Lascourreges, J.-F., Le Borgne, F., Le Goff, C., Magot, M., 2009. Characterization

719   by culture and molecular analysis of the microbial diversity of a deep subsurface

720   gas storage aquifer. Res. Microbiol. 160, 107–116.

721   doi:10.1016/j.resmic.2008.10.010

722 Bellagamba, M., Cruz Viggi, C., Ademollo, N., Rossetti, S., Aulenta, F., 2016. Electrolysis-

723   driven bioremediation of crude oil-contaminated marine sediments. N. Biotechnol.

724   doi:10.1016/j.nbt.2016.03.003

725 Borole, A.P., Reguera, G., Ringeisen, B., Wang, Z.-W., Feng, Y., Kim, B.H., 2011.

726   Electroactive biofilms: Current status and future research needs. Energy Environ.

727   Sci. 4, 4813. doi:10.1039/c1ee02511b

728 Callaghan, A. V., Davidova, I.A., Savage-Ashlock, K., Parisi, V.A., Gieg, L.M., Suflita, J.M.,

729   Kukor, J.J., Wawrik, B., 2010. Diversity of benzyl- and alkylsuccinate synthase genes

730   in hydrocarbon-impacted environments and enrichment cultures. Environ. Sci.

731   Technol. 44, 7287–7294. doi:10.1021/es1002023

732 Caporaso, J.G., Kuczynski, J., Stombaugh, J., Bittinger, K., Bushman, F.D., Costello, E.K.,

733   Fierer, N., Peña, A.G., Goodrich, J.K., Gordon, J.I., Huttley, G.A., Kelley, S.T., Knights, D.,

734   Koenig, J.E., Ley, R.E., Lozupone, C.A., McDonald, D., Muegge, B.D., Pirrung, M.,

735   Reeder, J., Sevinsky, J.R., Turnbaugh, P.J., Walters, W.A., Widmann, J., Yatsunenko, T.,

736   Zaneveld, J., Knight, R., 2010a. QIIME allows analysis of high-throughput community

737   sequencing data. Nat. Methods 7, 335–336. doi:10.1038/nmeth.f.303

738 Caporaso, J.G., Bittinger, K., Bushman, F.D., DeSantis, T.Z., Andersen, G.L., Knight, R.,

739   2010b. PyNAST: a flexible tool for aligning sequences to a template alignment.

740   Bioinformatics 26, 266–267. doi:10.1093/bioinformatics/btp636

741 Conrad, R., Schink, B., Phelps, T.J., 1986. Thermodynamics of H2-consuming and H2-

742   producing metabolic reactions in diverse methanogenic environments under in situ

743   conditions. FEMS Microbiol. Lett. 38, 353–360. doi:10.1016/0378-1097(86)90013-

744   3

745 Daghio, M., Vaiopoulou, E., Patil, S.A., Suárez-Suárez, A., Head, I.M., Franzetti, A., Rabaey,

746   K., 2016. Anodes stimulate anaerobic toluene degradation via sulfur cycling in

747   marine sediments. Appl. Environ. Microbiol. 82, 297–307. doi:10.1128/AEM.02250-

748   15

749 DeSantis, T.Z., Hugenholtz, P., Larsen, N., Rojas, M., Brodie, E.L., Keller, K., Huber, T.,

750   Dalevi, D., Hu, P., Andersen, G.L., 2006. Greengenes, a Chimera-Checked 16S rRNA

751   Gene Database and Workbench Compatible with ARB. Appl. Environ. Microbiol. 72,

752   5069–5072. doi:10.1128/AEM.03006-05

753 Edgar, R.C., 2010. Search and clustering orders of magnitude faster than BLAST.

754   Bioinformatics 26, 2460–2461. doi:10.1093/bioinformatics/btq461

755 Fazi, S., Aulenta, F., Majone, M., Rossetti, S., 2008. Improved quantification of

756   Dehalococcoides species by fluorescence in situ hybridization and catalyzed

757   reporter deposition. Syst. Appl. Microbiol. 31, 62–67.

758   doi:10.1016/j.syapm.2007.11.001

759 Genovese, M., Crisafi, F., Denaro, R., Cappello, S., Russo, D., Calogero, R., Santisi, S.,

760   Catalfamo, M., Modica, A., Smedile, F., Genovese, L., Golyshin, P.N., Giuliano, L.,

761   Yakimov, M.M., 2014. Effective bioremediation strategy for rapid in situ cleanup of

762   anoxic marine sediments in mesocosm oil spill simulation. Front. Microbiol. 5.

763   doi:10.3389/fmicb.2014.00162

764   Gray, N.D., Sherry, A., Grant, R.J., Rowan, A.K., Hubert, C.R.J., Callbeck, C.M., Aitken, C.M.,

765   Jones, D.M., Adams, J.J., Larter, S.R., Head, I.M., 2011. The quantitative significance of

766   Syntrophaceae and syntrophic partnerships in methanogenic degradation of crude

767   oil alkanes. Environ. Microbiol. 13, 2957–2975. doi:10.1111/j.1462-

768   2920.2011.02570.x

769   Haas, B.J., Gevers, D., Earl, A.M., Feldgarden, M., Ward, D. V., Giannoukos, G., Ciulla, D.,

770   Tabbaa, D., Highlander, S.K., Sodergren, E., Methé, B., DeSantis, T.Z., Petrosino, J.F.,

771   Knight, R., Birren, B.W., 2011. Chimeric 16S rRNA sequence formation and detection

772   in Sanger and 454-pyrosequenced PCR amplicons. Genome Res. 21, 494–504.

773   doi:10.1101/gr.112730.110

774   Hagen, L.H., Vivekanand, V., Linjordet, R., Pope, P.B., Eijsink, V.G.H., Horn, S.J., 2014.

775   Microbial community structure and dynamics during co-digestion of whey

776   permeate and cow manure in continuous stirred tank reactor systems. Bioresour.

777   Technol. 171, 350–359. doi:10.1016/j.biortech.2014.08.095

778   Hasegawa, R., Toyama, K., Miyanaga, K., Tanji, Y., 2014. Identification of crude-oil

779   components and microorganisms that cause souring under anaerobic conditions.

780   Appl. Microbiol. Biotechnol. 98, 1853–1861. doi:10.1007/s00253-013-5107-3

781   Head, I.M., 1999. Recovery and analysis of ribosomal RNA sequences from the

782   environment, in: Edwards, C. (Ed.), Environmental Monitoring of Bacteria. Humana

783   Press, Totowa, New Jersey, pp. 139–174.

784   Head, I.M., Gray, N.D., Larter, S.R., 2014. Life in the slow lane; biogeochemistry of

785   biodegraded petroleum containing reservoirs and implications for energy recovery

786   and carbon management. Front. Microbiol. 5, 566. doi:10.3389/fmicb.2014.00566

787   Jones, D.M., Head, I.M., Gray, N.D., Adams, J.J., Rowan, A.K., Aitken, C.M., Bennett, B.,

788   Huang, H., Brown, A., Bowler, B.F.J., Oldenburg, T., Erdmann, M., Larter, S.R., 2008.

789   Crude-oil biodegradation via methanogenesis in subsurface petroleum reservoirs.

790   Nature 451, 176–180. doi:10.1038/nature06484

791   Kappell, A.D., Wei, Y., Newton, R.J., Van Nostrand, J.D., Zhou, J., McLellan, S.L., Hristova,

792   K.R., 2014. The polycyclic aromatic hydrocarbon degradation potential of Gulf of

793   Mexico native coastal microbial communities after the Deepwater Horizon oil spill.

794   Front. Microbiol. 5, 205. doi:10.3389/fmicb.2014.00205

795   King, G.M., Judd, C., Kuske, C.R., Smith, C., 2012. Analysis of Stomach and Gut

796   Microbiomes of the Eastern Oyster (Crassostrea virginica) from Coastal Louisiana,

797   USA. PLoS One 7, e51475. doi:10.1371/journal.pone.0051475

798   Klindworth, A., Pruesse, E., Schweer, T., Peplies, J., Quast, C., Horn, M., Glöckner, F.O.,

799   2013. Evaluation of general 16S ribosomal RNA gene PCR primers for classical and

800   next-generation sequencing-based diversity studies. Nucleic Acids Res. 41, e1.

801   doi:10.1093/nar/gks808

802   Koo, H., Mojib, N., Huang, J.P., Donahoe, R.J., Bej, A.K., 2015. Bacterial community shift in

803   the coastal Gulf of Mexico salt-marsh sediment microcosm in vitro following

804   exposure to the Mississippi Canyon Block 252 oil (MC252). 3 Biotech 5, 379–392.

805   doi:10.1007/s13205-014-0233-x

806   Kuivila, K.M., Murray, J.W., Devol, A.H., Novelli, P.C., 1989. Methane production, sulfate

807   reduction and competition for substrates in the sediments of Lake Washington.

808   Geochim. Cosmochim. Acta 53, 409–416. doi:10.1016/0016-7037(89)90392-X

809   Lee, J., Lee, T.K., Löffler, F.E., Park, J., 2011. Characterization of microbial community

810   structure and population dynamics of tetrachloroethene-dechlorinating tidal

811   mudflat communities. Biodegradation 22, 687–698. doi:10.1007/s10532-010-

812   9429-x

813   Lovley, D.R., Klug, M.J., 1986. Model for the distribution of sulfate reduction and

814   methanogenesis in freshwater sediments. Geochim. Cosmochim. Acta 50, 11–18.

815   doi:10.1016/0016-7037(86)90043-8

816 Lovley, D.R., Nevin, K.P., 2011. A shift in the current: New applications and concepts for

817   microbe-electrode electron exchange. Curr. Opin. Biotechnol.

818   doi:10.1016/j.copbio.2011.01.009

819 Matturro, B., Frascadore, E., Cappello, S., Genovese, M., Rossetti, S., 2016. In situ

820   detection of alkB2 gene involved in Alcanivorax borkumensis SK2T hydrocarbon

821   biodegradation. Mar. Pollut. Bull. 110, 378–382.

822   doi:10.1016/j.marpolbul.2016.06.038

823 Meckenstock, R.U., Safinowski, M., Griebler, C., 2004. Anaerobic degradation of polycyclic

824   aromatic hydrocarbons, in: FEMS Microbiology Ecology. pp. 27–36.

825   doi:10.1016/j.femsec.2004.02.019

826 Miura, Y., Okabe, S., 2008. Quantification of cell specific uptake activity of microbial

827   products by uncultured Chloroflexi by microautoradiography combined with

828   fluorescence in situ hybridization. Environ. Sci. Technol. 42, 7380–6.

829   doi:10.1021/es800566e

830 Morris, J.M., Jin, S., Crimi, B., Pruden, A., 2009. Microbial fuel cell in enhancing anaerobic

831   biodegradation of diesel. Chem. Eng. J. doi:10.1016/j.cej.2008.05.028

832 O'Sullivan, L.A., Roussel, E.G., Weightman, A.J., Webster, G., Hubert, C.R.J., Bell, E., Head, I.,

833   Sass, H., Parkes, R.J., 2015. Survival of Desulfotomaculum spores from estuarine

834   sediments after serial autoclaving and high-temperature exposure. ISME J. 9, 922–

835   33. doi:10.1038/ismej.2014.190

836 Oremland, R.S., Polcin, S., 1982. Methanogenesis and sulfate reduction: competitive and

837   noncompetitive substrates in estuarine sediments. Appl. Environ. Microbiol. 44,

838   1270–1276. doi:10.1016/0198-0254(83)90262-5

839   Oremland, R.S., Taylor, B.F., 1978. Sulfate reduction and methanogenesis in marine

840   sediments. Geochim. Cosmochim. Acta 42, 209–214. doi:10.1016/0016-

841   7037(78)90133-3

842   Paulo, L.M., Stams, A.J.M., Sousa, D.Z., 2015. Methanogens, sulphate and heavy metals: a

843   complex system. Rev. Environ. Sci. Bio/Technology 14, 537–553.

844   doi:10.1007/s11157-015-9387-1

845   Quince C, Lanzen A, Davenport R, Turnbaugh P (2011) Removing noise from

846   pyrosequenced amplicons. BMC Bioinform 12, 38. doi:10.1186/1471-2105-12-38

847   Ravot, G., Magot, M., Fardeau, M.-. L., Patel, B.K., Thomas, P., Garcia, J.-. L., 1999.

848   Fusibacter paucivorans gen. nov., sp. nov., an anaerobic, thiosulfate-reducing

849   bacterium from an oil-producing well. Int J Syst Bacteriol 49, 1141–1147.

850   doi:10.1099/00207713-49-3-1141

851   Reis, M., Almeida, J.S., Lemos, P.C., Carrondo, M.J., 1992. Effect of hydrogen sulfide on

852   growth of sulfate reducing bacteria. Biotechnol. Bioeng. 40, 593–600.

853   doi:10.1002/bit.260400506

854   Sanni, G.O., Coulon, F., McGenity, T.J., 2015. Dynamics and distribution of bacterial and

855   archaeal communities in oil-contaminated temperate coastal mudflat mesocosms.

856   Environ. Sci. Pollut. Res. 22, 15230–15247. doi:10.1007/s11356-015-4313-1

857   Savage, K.N., Krumholz, L.R., Gieg, L.M., Parisi, V.A., Suflita, J.M., Allen, J., Philp, R.P.,

858   Elshahed, M.S., 2010. Biodegradation of low-molecular-weight alkanes under

859   mesophilic, sulfate-reducing conditions: metabolic intermediates and community

860   patterns. FEMS Microbiol. Ecol. 72, 485–495. doi:10.1111/j.1574-

861   6941.2010.00866.x

862   Sherry, A., Grant, R.J., Aitken, C.M., Jones, D.M., Head, I.M., Gray, N.D., 2014. Volatile

863   hydrocarbons inhibit methanogenic crude oil degradation. Front. Microbiol. 5.

864   doi:10.3389/fmicb.2014.00131

865   Sherry, A., Gray, N.D., Ditchfield, A.K., Aitken, C.M., Jones, D.M., Röling, W.F.M., Hallmann,

866   C., Larter, S.R., Bowler, B.F.J., Head, I.M., 2013a. Anaerobic biodegradation of crude

867   oil under sulphate-reducing conditions leads to only modest enrichment of

868   recognized sulphate-reducing taxa. Int. Biodeterior. Biodegrad. 81, 105–113.

869   doi:10.1016/j.ibiod.2012.04.009

870   Sherry, A., Gray, N.D., Ditchfield, A.K., Aitken, C.M., Jones, D.M., Röling, W.F.M., Hallmann,

871   C., Larter, S.R., Bowler, B.F.J., Head, I.M., 2013b. Anaerobic biodegradation of crude

872   oil under sulphate-reducing conditions leads to only modest enrichment of

873   recognized sulphate-reducing taxa. Int. Biodeterior. Biodegrad. 81, 105–113.

874   doi:10.1016/j.ibiod.2012.04.009

875   Skennerton, C.T., Haroon, M.F., Briegel, A., Shi, J., Jensen, G.J., Tyson, G.W., Orphan, V.J.,

876   2016. Phylogenomic analysis of Candidatus "Izimaplasma" species: free-living

877   representatives from a Tenericutes clade found in methane seeps. ISME J. 10, 2679–

878   2692. doi:10.1038/ismej.2016.55

879   Spormann, A.M., Widdel, F., 2000. Metabolism of alkylbenzenes, alkanes, and other

880   hydrocarbons in anaerobic bacteria. Biodegradation 11, 85–105.

881   doi:10.1023/A:1011122631799

882   Sun, L., Liu, T., Müller, B., Schnürer, A., 2016. The microbial community structure in

883   industrial biogas plants influences the degradation rate of straw and cellulose in

884   batch tests. Biotechnol. Biofuels 9, 128. doi:10.1186/s13068-016-0543-9

885   Takii, S., Hanada, S., Tamaki, H., Ueno, Y., Sekiguchi, Y., Ibe, A., Matsuura, K., 2007.

886   Dethiosulfatibacter aminovorans gen. nov., sp. nov., a novel thiosulfate-reducing

887   bacterium isolated from coastal marine sediment via sulfate-reducing enrichment

888   with Casamino acids. Int. J. Syst. Evol. Microbiol. 57, 2320–2326.

889   doi:10.1099/ijs.0.64882-0

890   Viggi, C.C., Presta, E., Bellagamba, M., Kaciulis, S., Balijepalli, S.K., Zanaroli, G., Papini, M.P.,

891   Rossetti, S., Aulenta, F., 2015. The "Oil-Spill Snorkel": An innovative

892   bioelectrochemical approach to accelerate hydrocarbons biodegradation in marine

893   sediments. Front. Microbiol. 6. doi:10.3389/fmicb.2015.00881

894   von Netzer, F., Pilloni, G., Kleindienst, S., Krüger, M., Knittel, K., Gründger, F., Luedersa, T.,

895   2013. Enhanced gene detection assays for fumarate-adding enzymes allow

896   uncovering of anaerobic hydrocarbon degraders in terrestrial and marine systems.

897   Appl. Environ. Microbiol. 79, 543–552. doi:10.1128/AEM.02362-12

898   Wang, Q., Garrity, G.M., Tiedje, J.M., Cole, J.R. 2007. Naïve Bayesian classifier for rapid

899   assignment of rRNA sequences into the new bacterial taxonomy. Appl. Environ.

900   Microbiol. 73, 5261-5267. doi:10.1128/AEM.00062-07

901   Wang, H., Ren, Z.J., 2013. A comprehensive review of microbial electrochemical systems

902   as a platform technology. Biotechnol. Adv. 31, 1796–1807.

903   doi:10.1016/j.biotechadv.2013.10.001

904   Yamada, T., Sekiguchi, Y., 2009. Cultivation of uncultured chloroflexi subphyla:

905   significance and ecophysiology of formerly uncultured chloroflexi "subphylum i"

906   with natural and biotechnological relevance. Microbes Environ. 24, 205–216.

907   doi:10.1264/jsme2.ME09151S

908   Yamada, T., Sekiguchi, Y., Hanada, S., Imachi, H., 2006. Anaerolinea thermolimosa sp.

909   nov., Levilinea saccharolytica gen. nov., sp. nov. and Leptolinea tardivitalis gen. nov.,

910   sp. nov., novel filamentous anaerobes, and description of the new classes

911   Anaerolineae classis nov. and Caldilineae classis nov. in the. Int. J. Syst. Evol.

912   Microbiol. 56, 1331–1340. doi:10.1099/ijs.0.64169-0

913   Yan, F., Reible, D., 2014. Electro-bioremediation of contaminated sediment by electrode

914   enhanced capping. J. Environ. Manage. 155, 154–161.

915   doi:10.1016/j.jenvman.2015.03.023

916   Zhang, F., Cheng, S., Pant, D., Bogaert, G. Van, Logan, B.E., 2009. Power generation using

917   an activated carbon and metal mesh cathode in a microbial fuel cell. Electrochem.

918   commun. 11, 2177–2179. doi:10.1016/j.elecom.2009.09.024

919